ordinary progress in the field of oligosaccharide and glycopeptide synthesis. Given the extendibility of this chemistry to virtually any type of saccharide presentation and the capacity, in principle, for ligation of the pentapeptide construct to larger polypeptide or protein domains,[24] the synthesis of sequence-defined homogeneous glycopeptides, and thence glycoproteins, is at hand. Studies directed toward reaching fully functional glycoproteins by total synthesis are underway.

Received: January 22, 2001 [Z16470]

[1] a) P. Burda, M. Aebi, *Biochem. Bioophys. Acta* **1999**, *1426*, 239; b) R. A. Dwek, *Chem. Rev.* **1996**, *96*, 683; c) R. A. Dwek, *Science* **1995**, *269*, 1234; d) A. Varki, *Glycobiology* **1993**, *3*, 97.

[2] a) S. E. O'Connor, B. Imperiali, *Chem. Biol.* **1996**, *3*, 803; b) B. Imperiali, S. E. O'Connor, *Curr. Opin. Chem. Biol.* **1999**, *3*, 643.

[3] L. H. Shevinsky, B. B. Knowles, I. Damjanov, D. Solter, *Cell* **1982**, *30*, 697.

[4] a) W. Van Dijk, G. A. Turner, A. Mackiewicz, *Glycosyl. Dis.* **1994**, *1*, 5; b) W. Van Dijk, M. E. Van der Stelt, A. Salera, L. Dente, *Eur. J. Cell Biol*. **1991**, *55*, 143.

[5] a) A. Kobata, *Acc. Chem. Res.* **1993**, *26*, 319; b) T. Feizi, *Nature* **1985**, 314, 53.

[6] A. Varki, R. Cummings, J. Esko, H. Freeze, G. Hart, J. Marth, *Essentials of Glycobiology*, Cold Spring Harbor Laboratory Press, Cold Spring Harbor, **1999**.

[7] a) J. N. Beitter, R. E. Means, R. C. Desrosiers, *Nat. Med.* **1998**, *4*, 678; b) K. O. Lloyd, *Am. J. Clin. Pathol.* **1987**, *87*, 129.

[8] "The Molecular Basis of Blood Diseases": J. B. Lowe in *Red Cell Membrane Antigens* (Eds.: G. Stamatoyannopoulos, A. W. Nienhutis, P. W. Majeruis, H. Varmus), Saunders, Philadelphia, **1994**, pp. 293–330.

[9] For a review on the syntheses of O- and N-linked glycopeptides, see: a) G. Arsequell, G. Valencia, *Tetrahedron: Asymmetry* **1997**, *8*, 2839; b) G. Arsequell, G. Valencia, *Tetrahedron: Asymmetry* **1999**, *10*, 3045. For examples of chemical and chemoenzymatic syntheses of high mannose linked glycopeptides, see: c) I. Matsuo, Y. Nakahara, Y. Ito, T. Nukuda, V. Nakara, T. Ogawa, *Bioorg. Med. Chem*. **1995**, *3*, 1455; d) Y. Ito, T. Ogawa, *J. Am. Chem. Soc.* **1997**, *119*, 5562; e) Z. W. Guo, Y. Nakahara, T. Ogawa, *Angew. Chem.* **1997**, *109*, 1527; *Angew. Chem. Int. Ed.* **1997**, *36*, 1464; f) C. Unverzagt, *Carb. Res.* **1998**, *305*, 423; g) C. Unverzagt, *Angew. Chem.* **1997**, *109*, 2078; *Angew. Chem. Int. Ed. Engl.* **1997**, *36*, 1989; C. Unverzagt, *Angew. Chem.* **1996**, *108*, 2507; *Angew. Chem. Int. Ed. Engl.* **1996**, *35*, 2350; C. Unverzagt, *Angew. Chem.* **1994**, *106*, 1170; *Angew. Chem. Int. Ed. Engl.* **1994**, *33*, 1102; h) M. Mitzuno, K. Handa, R. Iguchi, I. Muramoto, T. Kawakami, S. Aimoto, K. Yamammoto, T. Inazu, *J. Am. Chem. Soc.* **1999**, *121*, 284; i) R. R. Schmidt, R. R. Kinzy, *Adv. Carbohydr. Chem. Biochem.* **1994**, *50*, 21.

[10] For a definition of glycoprotein classification and nomenclature, see: J. F. G. Vliegenthart, J. Montreuil, *Glycoproteins* (Eds.: J. F. G. Vliegenthart, J. Montreuil, H. Schachter), Elsevier, New York, **1995**, pp. 13–28.

[11] For an earlier version of the general strategy we employed to reach the high mannose core system, see: P. H. Seeberger, P. F. Cirillo, S. Hu, X. Beebe, M. T. Bilodeau, S. J. Danishefsky, *Enantiomer* **1996**, *1*, 311.

[12] S. J. Danishefsky, S. Hu, P. F. Cirillo, M. Eckhardt, P. H. Seeberger, *Chem. Eur. J.* **1997**, *3*, 1617.

[13] a) P. Seeberger, M. Eckhardt, C. Gutteridge , S. J. Danishefky, *J. Am. Chem. Soc.* **1997**, *119*, 10064; b) Z. G. Wang, X. Zhang, D. Live, S. J. Danishefsky, *Angew. Chem.* **2000**, *112*, 3798; *Angew. Chem. Int. Ed.* **2000**, *39*, 3652.

[14] With modification of the original procedure from: M. A. E. Shaban, R. W. Jeanloz, *Carbohydr. Res.* **1976**, *46*, 138.

[15] a) R. Gigg, *Am. Chem. Soc. Symp. Ser.* **1977**, *39*, 253; b) Z. G. Wang, Y. Ito, Y. Nakahara, T.Ogawa, *Bioorg. Med. Chem. Lett.* **1994**, *4*, 2805.

[16] S. J. Danishefsky, K. Koseki, D. A. Griffith, J. Gervay, J. M. Peterson, F. E. McDonald, T. Oriyama, *J. Am. Chem. Soc.* **1992**, *114*, 8331.

[17] Piv_2O (or Ac_2O) is needed to dehydrate the initial adduct (amide) into the phthalimide **10**.

[18] a) T. Sasaki, K. Minamoto, H. Itoh, *J. Org. Chem*. **1978**, *43*, 2320; b) Z. G. Wang, X. F. Zhang, Y. Ito, Y. Nakahara, T. Ogawa, *Carbohydr. Res.* **1996**, *295*, 25.

[19] For a recent example featuring simultaneous removal of 17 benzyl groups, see: W. Frick, A. Bauer, J. Bauer, S. Wied, G. Müller, *Biochemistry* **1998**, *37*, 13421.

[20] a) L. M. Likhosherstov, O. S. Novikova, V. A. Derevitskaja, N. K. Kochetkov, *Carbohydr. Res.* **1986**, *146*, C1; b) S. T. Cohen-Anisfeld, P. T. Lansbury, Jr., *J. Am. Chem. Soc.* **1993**, *115*, 10531.

[21] HBTU/HOBt: a) R. Knorr, A. Trzeciak, W. Bannwarth, D. Gillessen, *Tetrahedron Lett.* **1989**, *30*, 1927; b) A. Speicher, T. Klaus, T. Eicher, *J. Prakt. Chem.* **1998**, *340*, 581.

[22] Analysis of the fine specificities of 11 mouse monoclonal antibodies reactive with H-type 2 blood group determinants: K. Furukawa, S. Welt, B. W. T. Yin, H.-J. Feickert, T. Takahashi, R. Ueda, K. O. Lloyd, *Mol. Immunol.* **1990**, *27*, 723.

[23] Actually, these data demonstrate that, at the least, one of the two H-type 2 determinants in **1** is immunorecognized. They do not prove that *both* H-type subunits in **1** are recognized, although this is presumably the case.

[24] a) P. E. Dawson, T. W. Muir, I. Clark-Lewis, S. B. H. Kent, *Science* **1994**, *266*, 776; reviews: b) G. J. Cotton, T. W. Muir, *Chem. Biol.* **1999**, *6*, R247; c) L. A. Marcaurelle, C. R. Bertozzi, *Chem. Eur. J.* **1999**, *5*, 1384; d) G. G. Kochendoerfer, S. B. H. Kent, *Curr. Opin. Chem. Biol.* **1999**, *3*, 665.

Enhanced Physical Properties in a Pentacene Polymorph

Theo Siegrist,* Christian Kloc, Jan H. Schön, Bertram Batlogg, Robert C. Haddon, Steffen Berg, and Gordon A. Thomas

Pentacene is a highly promising material for application in thin film transistor devices because of its recently reported high mobilities and good semiconducting behavior.[1] For this reason, we have carried out a program to grow single crystals of unusually high purity and crystalline perfection to study the intrinsic properties of organic semiconductors. We have produced millimeter-sized crystals with electrically active impurities at concentrations of the order of 10^{13} cm^{-3} (or one impurity molecule per 10^8 pentacene molecules) by using a vapor-phase deposition technique. Such crystals were used for

[*] Prof. Dr. T. Siegrist,[+] Dr. C. Kloc, Dr. J. H. Schön, Prof. Dr. B. Batlogg,[++] S. Berg, Prof. Dr. G. A. Thomas
Bell Laboratories, Lucent Technologies
600 Mountain Avenue, Murray Hill, NJ 07974 (USA)
Fax: (+1) 908-582-2521
E-mail: tsi@bell-labs.com
Prof. Dr. R. C. Haddon
Departments of Chemistry and Physics
and Advanced Carbon Materials Center
University of Kentucky, Lexington, KY 40506-0055 (USA)
[+] Other address:
Inorganic Chemistry 2, Lund University (Sweden)
[++] Other address:
Institute of Solid State Physics, ETH Zürich (Switzerland)

  1433-7851/01/4009-1732 $ 17.50+.50/0

a crystal structure determination, optical absorption, and electrical transport measurements. A new polymorph of pentacene was identified, with a slightly higher density than the solution-grown phase previously reported.[2, 3] The new structure leads to a large number of carbon–carbon contacts within the range of 3.6 to 4.0 Å (Figure 1). However, the average carbon–carbon distances are similar in both modifications and are larger than the sum of the van der Waals spacing for pairs of carbon atoms.

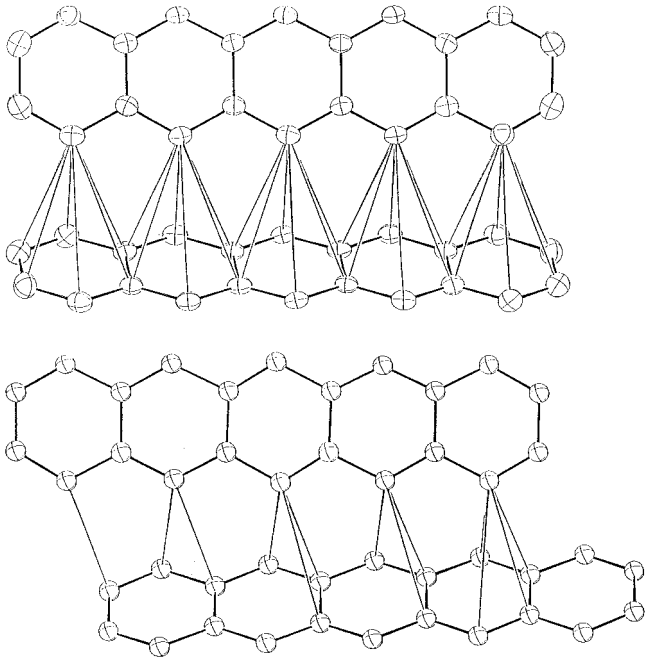

Figure 1. Top: Molecular arrangement of pentacene(vapor). Bottom: Molecular arrangement of pentacene(solution). In both diagrams the lines connecting molecules indicate the intermolecular carbon–carbon contacts within the range of 3.5 to 3.92 Å.

The small differences in the molecular packing affect the electrical properties, and enhance the carrier mobility in the vapor-phase-grown polymorph. Similar effects have previously been observed in thiophenes, where the high-temperature polymorph showed enhanced carrier mobility over the low-temperature polymorph.[4]

Structural studies on single crystals of pentacene have previously been carried out only on solution-grown single crystals obtained from trichlorobenzene solutions.[2, 3] The lattice constants of the solution-grown crystals were given as $a = 7.90$, $b = 6.06$, $c = 16.01$ Å, $\alpha = 101.9$, $\beta = 112.6$, $\gamma = 85.8^\circ$, which gives a (001) d-spacing of 14.5 Å. In contrast, the X-ray diffraction pattern of vacuum-deposited thin films often show an elongated (001) d-spacing of 15.5 Å as well as the expected 14.5 Å spacing.[5, 6] Therefore, the structure of solution-grown pentacene crystals is expected to differ from vapor-grown crystals and thin films. Polymorphism is quite often observed in molecular crystals, where different preparation techniques can produce different molecular packing[7] depending on the pressure, substrate temperature, carrier-gas flow, and other variables. As a consequence, the bulk physical properties also depend strongly on the molecular arrangement, as has been found, for example, for the polymorphic forms of α-quaterthiophene (α-4T) and α-hexathiophene (α-6T).[7–9] The highest mobilities were observed in the high temperature polymorphs of these materials. We infer a similar effect among the polymorphs grown by the thin-film method and other syntheses of pentacene.

The unit cell obtained for the vapor-phase-grown pentacene (pentacene(vapor)) is similar, but not identical, to the solution-grown pentacene (pentacene(solution)) reported previously.[2, 3] The space group is the same for both, namely $P\bar{1}$, with $Z = 2$. The unit cell for vapor-grown pentacene contains two crystallographically independent molecules which are expected to be chemically identical. The unit cell for pentacene(solution) is $a = 7.90$, $b = 6.06$, $c = 16.01$ Å, $\alpha = 101.9$, $\beta = 112.6$, $\gamma = 85.8^\circ$ and reduces to $a = 6.06$, $b = 7.90$, $c = 14.88$ Å, $\alpha = 96.74$, $\beta = 100.54$, $\gamma = 94.2^\circ$. This reduced cell can now be compared to the one of pentacene(vapor): $a = 6.253$, $b = 7.786$, $c = 14.511$ Å, $\alpha = 76.65$, $\beta = 87.50$, $\gamma = 84.6^\circ$. Clearly, the angles differ whereas the unit cell lengths are quite similar. In fact, the volume of the unit cell of pentacene(vapor) is reduced by about 3% over pentacene(solution), and results in slightly denser molecular packing. This is also reflected in the number of average contacts (Figure 1). If a contact distance of up to 4 Å is considered, there are 5.36 contacts per carbon atom in pentacene(vapor) versus 4 contacts per carbon atom in pentacene(solution). If the cutoff is set at 3.9 Å, then the values are 4.1 contacts per carbon atom for pentacene(vapor) versus 2.5 contacts per carbon atom for pentacene(solution). The two polymorphs can be distinguished by measuring the d-spacing of the (001) reflection: it is 14.5 Å for pentacene(solution) and 14.1 Å for pentacene(vapor). The differences in the arrangements are quite subtle. While the herringbone-type arrangement of the molecules is present in both polymorphs, the molecules are shifted against each other differently. This effect is seen in Figure 1, where the intermolecular contacts are indicated by thin lines for carbon–carbon contacts shorter than 3.92 Å. The observed d-spacing cannot explain some of the elongated d-spacings observed in thin films. More polymorphic arrangements are therefore expected. A recent study of planar organic systems[10] confirmed the unit cell found for pentacene.

Optical spectra of the crystals were recorded over the frequency range from the far-infrared to the near ultraviolet. A Fourier-transform spectrometer was used for the far-infrared region, and a grating spectrometer was used for the visible and near-ultraviolet regions. The samples were held in a strain-free apparatus at room temperature. The crystals were small flat needles, so the light was directed onto the large face and was polarized along and perpendicular to the crystals' longest axis. Several crystals with typical dimensions of $5\ \text{mm} \times 1\ \text{mm} \times 10\ \mu\text{m}$ were analyzed. Since there was substantial uncertainty in the value of the thin dimension, results for the absorbance are presented in arbitrary units. The optical results are shown in Figure 2. Figure 2a and b show the negative log of the transmitted intensity as a function of the photon energy in the region of the molecular vibrational modes, which appear as a series of sharp, asymmetric lines. A comparison of the vibrational mode energies with those in similar compounds[11]

  1433-7851/01/4009-1733 $ 17.50+.50/0

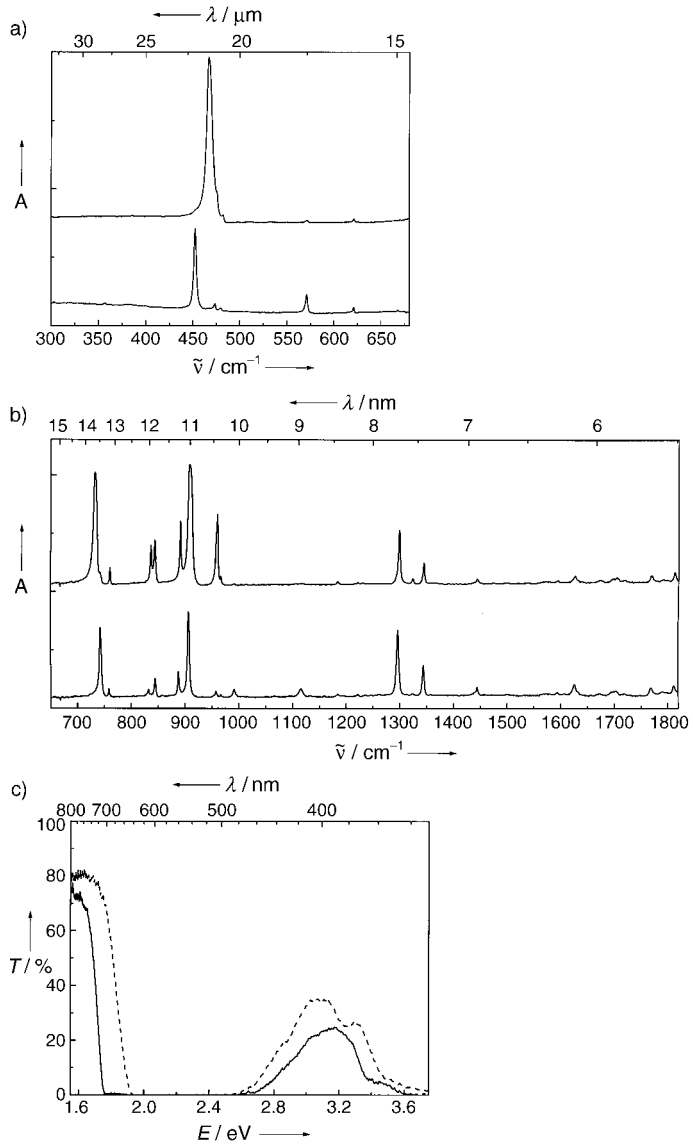

Figure 2. a) Relative absorbance as defined by the negative log of the transmitted intensity as a function of the energy of the light. The two curves are for different polarizations of the light as indicated. b) Same data as in part (a) but for higher photon energies. c) Transmitted intensity as a function of photon energy (in eV) showing the wide absorption between 1.8 and 3.0 eV.

shows that these peaks are typical of this class of material and shift according to the molecular structure. Although we have not measured the optical properties of the solution-grown crystals, a comparison with the results from similar compounds indicates that the lines will also shift, which is in keeping with the differences in the crystal structure.[11] Figure 2c shows the transmitted intensity on a linear scale in the higher energy region, where two broad absorption features are seen near 2–3 eV and above 3.5 eV. These features show the presence of two types of excitations with strong dipole moments. The transitions between the valence and conduction bands generally have relatively weak absorption strengths relative to the excitonic excitations, as observed in many aromatic molecular crystals. However, when the broad observed absorption features and the high mobilities are considered together, the data suggest relatively broad conduction and valence bands in the energy range of the observed absorption features.

We have used space-charge-limited current (SCLC) spectroscopy, which has been found to be a powerful tool for studying the electrical properties of high-quality organic single crystals with low trap densities, to further study the crystals.[4] Thermoprobe measurements revealed that holes are the major charge carriers in as-grown pentacene. Moreover, gold contacts ensured unipolar transport. We found the transport in the pentacene crystals to be anisotropic, with a higher mobility for conduction parallel to the growth surface than perpendicular to the layered molecular structure. We have focused on data for charge transport along the direction of high mobility. The current–voltage characteristics in an applied electric field over many orders of magnitude ($10-4\times10^5\,V\,cm^{-1}$) exhibit four well-pronounced regimes[4] (Figure 3a). At low electric fields the current flow is ohmic and

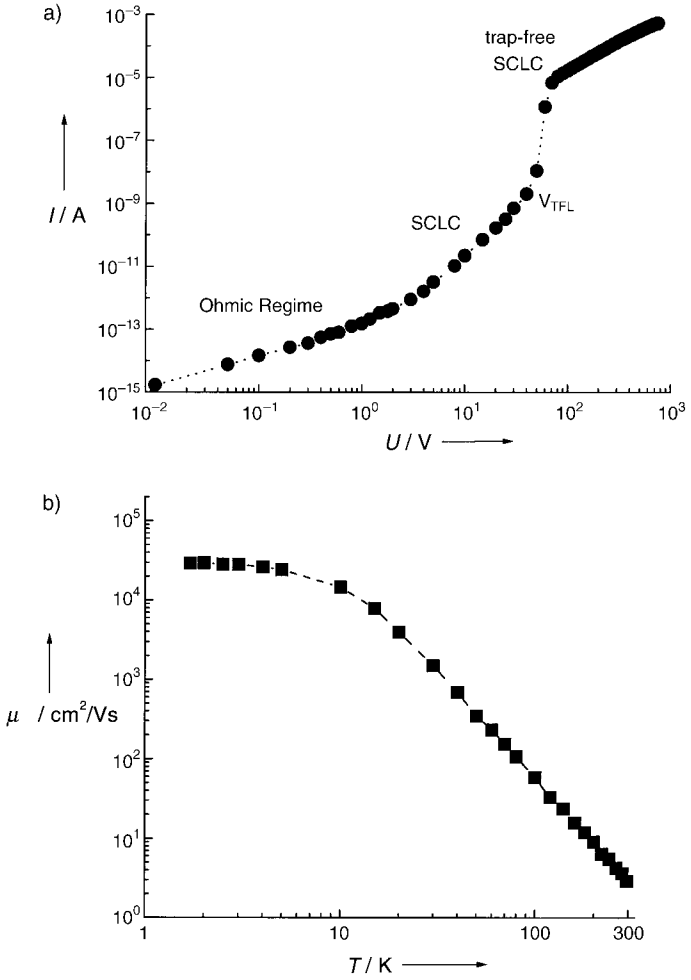

Figure 3. a) Current density versus applied electric field in the direction of high mobility for a high-quality single crystal of pentacene at room temperature. The current density initially follows Ohm's law at low electric fields and then becomes limited by space charge. If the injected carrier density exceeds the trap concentration, the traps are filled and the trap-free SCLC is observed. b) Charge carrier mobility in a hydrogen-annealed single crystal of pentacene as a function of temperature.

  1433-7851/01/4009-1734 $ 17.50+.50/0

becomes trap and space-charge limited. With increasing field strength, all the traps get filled and the mobility can be determined from the trap-free space charge-limited-current (SCLC) densities (j_{SCLC}) using Child's law if unipolar transport is assumed [Eq. (1)].

$$j_{SCLC} = \frac{9}{8}\frac{\varepsilon_r \varepsilon_0}{d^3}\mu V^2 \quad (1)$$

ε_0 is the permittivity of the free space, ε_r the relative dielectric constant, d the electrode distance, and V the applied voltage. Therefore, the hole mobility can be calculated from the trap-free SCLC. The temperature dependence of the mobility for a hydrogen-annealed (24 h at 200 °C) sample is shown in Figure 3b. The mobility increases as a power law from 3 $cm^2V^{-1}s^{-1}$ at room temperature as the temperature decreases. Mobilities as high as 10000 $cm^2V^{-1}s^{-1}$ are reached at low temperature. This behavior suggests there is bandlike charge transport in this organic semiconductor.

The mobility observed in pentacene is similar to the (charge-injection) mobilities that are seen in other benzenoid hydrocarbons at room temperature.[12, 13] However, it is not widely recognized that the mobilities in benzenoid hydrocarbons can be very large at low temperature, even though most of these molecules are not stacked and do not show close contacts in the crystal lattice. Room temperature mobilities in the benzenoid hydrocarbons can reach a few $cm^2V^{-1}s^{-1}$, but can increase by several orders of magnitude at low temperatures.[13] The bandwidths of these materials are calculated from extended Hückel theory (EHT) to be extremely narrow. The room-temperature mobility for pentacene is 3.0 $cm^2V^{-1}s^{-1}$, but extended Hückel calculations of the band dispersions give very narrow bands. Clearly extended Hückel calculations do not indicate a mechanism responsible for the observed high mobilities and, therefore, are not adequate to account for them in this system.

In conclusion, a new polymorphic form of pentacene that shows high mobilities and a low number of defects was grown as single crystals. The intrinsic physical properties of this new material were assessed, and showed charge carrier mobilities exceeding 10^4 $cm^2V^{-1}s^{-1}$ at low temperatures. Solar cells made from this material have already been shown[14] to give much higher efficiency than previously thought possible for an organic system. Furthermore, ambipolar field-effect transistors have been fabricated[15] that have relied on the crystal quality possible for this polymorph.

Experimental Section

Single crystals of pentacene were grown by physical vapor phase transport in an apparatus similar to that described earlier.[9] The source materials were obtained from Aldrich. Since vapor-phase transport in an open system is an efficient way of purification, multiple sublimations were carried out inside a crystal-growth reactor. A sample of 10 to 20 mg of pentacene was placed in a short tube (both sides open) inside a two-zone horizontal furnace and was exposed to either an Ar, He, H_2, or forming gas stream with a flow-rate of 40 – 100 mL min^{-1}. The pure gas, at a pressure of about 1 atm, was delivered to one end of the crystal-growth reactor and exited from the system through a bubbler, thus removing impurities and decomposition products. We found that pentacene is transported by convection under transport conditions similar to that used for the crystal growth of α-6T.[9] Thin crystals in the form of lamellae up to 10 mm long and 1 – 3 mm wide nucleated spontaneously on the reactor wall and grew concentric to the center of the reactor. Further steps include the annealing of the crystals to remove defects that influence charge transport in the material.

The structure of the polymorphic modification of pentacene was determined by X-ray diffraction. Integrated intensities were collected with graphite-monochromatized $Cu_{K\alpha}$ radiation on an Enraf – Nonius CAD-4 diffractometer, and the crystallographic analysis was carried out using the NRCVAX structure package.[16] The carbon atoms were refined anisotropically, while the hydrogen atoms were refined with a common isotropic temperature factor. No other constraints were applied. Pentacene ($C_{22}H_{14}$): dimensions $0.18 \times 0.10 \times 0.80$ mm, radiation $Mo_{K\alpha}$, space group $P\bar{1}$ (No. 2), $a = 6.265(2)$, $b = 7.786(2)$, $c = 14.511(4)$ Å, $\alpha = 76.65(1)$, $\beta = 87.50(2)$, $\gamma = 84.61(2)$, $V = 684.2(6)$ Å^3; $\rho_{calcd} = 1.35$ g cm^{-3}, temperature = 22.5 °C, $\mu = 0.70$ cm^{-1}, absorption correction = Gaussian integration, transmission factors = 0.9918 to 0.9953, 2θ range = 1 – 50°, total reflections = 4308, unique reflections = 2153, observed reflections ($I > 2.5\sigma$) = 838, R_f (all reflections) = 0.072, R_w (all reflections) = 0.050. Crystallographic data (excluding structure factors) for the structure reported in this paper have been deposited with the Cambridge Crystallographic Data Centre as supplementary publication no. CCDC-145333. Copies of the data can be obtained free of charge on application to CCDC, 12 Union Road, Cambridge CB2 1EZ, UK (fax: (+44) 1223-336-033; e-mail: deposit@ccdc.cam.ac.uk).

The band structure of pentacene was calculated using extended Hückel theory (EHT). The calculations use a version of the EHT programs constructed by M.-H. Whangbo as discussed previously.[17] In both cases, the valence bands show little dispersion, which is consistent with the observed intermolecular carbon – carbon contacts above 3.6 Å. This value is longer than the van der Waals separation of two carbon atoms of 3.4 Å.

For the optical properties measurements we used several light sources (deuterium, quartz-halogen, glow-bar, and Hg-arc), beam splitters (quartz, CaF, and Mylar), and detectors (Silicon, InSb, HgCdTe, and bolometer) to cover the frequency range from the far-infrared to the near ultraviolet. We focused light from a Michelson interferometer onto the crystals, measured the transmitted intensity, and used Fourier-transform calculations to obtain spectra. We supplemented the Michelson measurements in the visible and near ultraviolet regions with additional measurements using a grating spectrometer.

For transport measurements electrical contacts on the as-grown surface of single crystals of pentacene were prepared by thermal evaporation of gold strips through a shadow mask. Hence, the charge transport within the molecular planes could be investigated. The contacted samples were annealed in hydrogen at 150 °C. Current – voltage characteristics were measured in the temperature range between 1.7 and 300 K using a high sensitivity electrometer.

Received: August 29, 2000
Revised: February 8, 2001 [Z15720]

[1] J. H.Schön, C. Kloc, B. Batlogg, *Science* **2000**, *288*, 2338.
[2] R. B. Campbell, J. M. Robertson, J. Trotter, *Acta Crystallogr* **1961**, *14*, 705.
[3] R. B. Campbell, J. M. Robertson, J. Trotter, *Acta Crystallogr.* **1962**, *15*, 289.
[4] J. H. Schön, C. Kloc, R. A. Laudise, B. Batlogg, *Phys. Rev. B* **1998**, *58*, 12952.
[5] C. D. Dimitrakopoulos, A. R. Brown, A. Pomp, *J. Appl. Phys.* **1996**, *80*, 2501.
[6] D. J. Gundlach, T. N. Jackson, D. G. Schlom, S. F. Nelson, *Appl. Phys. Lett.* **1999**, *74*, 3302.
[7] T. Siegrist, R. M. Fleming, R. C. Haddon, R. A. Laudise, A. J. Lovinger, H. E. Katz, P. M. Bridenbaugh, D. D. Davis, *J. Mater. Res.* **1995**, *10*, 2170.
[8] R. C. Haddon, T. Siegrist, R. M. Fleming, P. M. Bridenbaugh, R. A. Laudise, *J. Mater. Chem.* **1995**, *5*, 1719.

  1433-7851/01/4009-1735 $ 17.50+.50/0

[9] C. Kloc, P. Simpkins, T. Siegrist, R. A. Laudise, *J. Cryst. Growth* **1997**, *182*, 416.
[10] D. Holmes, S.Kumaraswamy, A. J. Matzger, K. P. C. Vollhardt, *Chem. Eur. J.* **1999**, *5*, 3399.
[11] S. Berg, A. Markelz, G. A. Thomas, J. H. Schön, C. Kloc, P. B. Littlewood, B. Batlogg, *Phys. Rev. B*, in press.
[12] N. Karl, J. Marktanner, R. Stehle, W. Warta, *Synth. Met.* **1991**, *41 – 43*, 2473.
[13] W. Warta, N. Karl, *Phys. Rev. A* **1985**, *36*, 136.
[14] J. H. Schön, C. Kloc, E. Bucher, B. Batlogg, *Nature* **2000**, *403*, 408.
[15] J. H. Schön, S. Berg, C Kloc, B. Batlogg, *Science* **2000**, *287*, 1022.
[16] E. J. Gabe, Y. Le Page, J.-P. Charland, F. L. Lee, P. S. White, *J. Appl. Cryst.* **1989**, *22*, 384.
[17] R. C. Haddon, A. P. Ramirez, S. H. Glarum, *Adv. Mater.* **1994**, *6*, 316; M. P. Andrews, A. W. Cordes, D. C. Douglass, R. M. Fleming, S. H. Glarum, R. C. Haddon, P. Marsh, R. T. Oakley, T. T. M. Palstra, L. F. Schneemeyer, G. W. Trucks, R. Tycko, J. V. Waszczak, K. M. Young, N. M. Zimmerman, *J. Am. Chem. Soc.* **1991**, *113*, 3559.

Total Synthesis of Azinomycin A**

Robert S. Coleman,* Jing Li, and Antonio Navarro

The azinomycins A and B (**1** and **2**; Ac = acetyl) are a functionally complex family of antitumor agents isolated from fermentation broths of *Streptomyces griseofuscus*.[1] These natural products are of synthetic interest because of the unprecedented and densely functionalized aziridino[1,2-*a*]pyrrolidine ring system; additional attention has been focused on these agents because of their potential as lead compounds for the design of novel chemotherapeutic agents.[2] To date, and despite considerable effort from a number of laboratories,[3] the total synthesis of these challenging targets has not been achieved. Herein, we describe an asymmetric total synthesis of azinomycin A (**1**) that represents the first entry into this family of natural products.

The azinomycins exhibit cytotoxity against at sub-microgram per milliliter concentrations, but, more important, these agents show antitumor activity in mouse models that is comparable to that of mitomycin C.[4] Unfortunately, a detailed evaluation of the scope of the biological activity of the native agents has been prevented by the poor availability and significant instability of the agents, factors that have similarly impeded synthetic efforts.

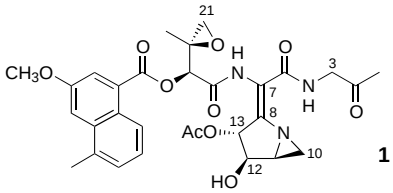

1

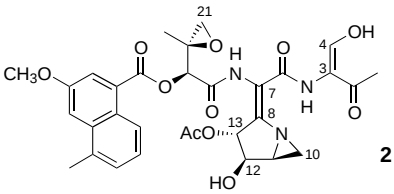

2

The azinomycins are one of a small set of molecules that interact with DNA in the major groove.[5] Azinomycin B (**2**) forms a covalent interstrand cross-link[6] between suitably disposed purine bases in the duplex sequence 5′-d(PuNPy)-3′, but the structural origin of the sequence selectivity and binding affinity are incompletely defined. We have recently described a computationally based model[7] that explains the experimentally observed cross-linking of azinomycin B (**2**).[8]

We now report the asymmetric total synthesis of azinomycin A (**1**) that is based on a convergent and modular synthetic plan (Scheme 1). By the five disconnections at ester, amide,

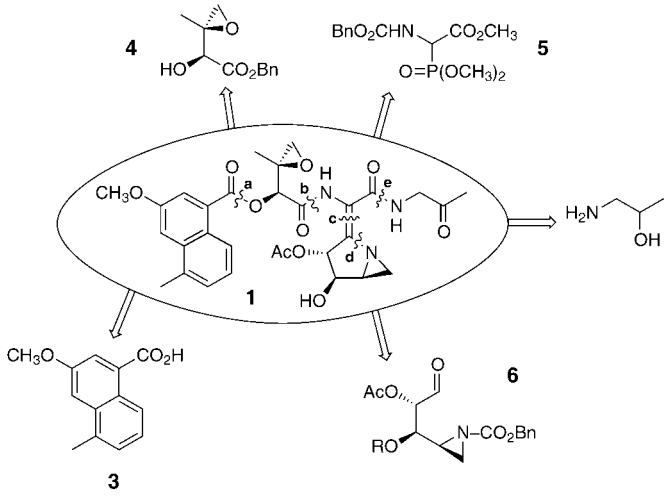

Scheme 1. Modular and convergent synthetic strategy. Bn = benzyl.

olefin and C–N bonds, a – e, we arrive retrosynthetically at five simple fragments: 1) naphthoic acid **3**,[2q] 2) epoxyalcohol **4**,[9] 3) glycine phosphonate **5**,[10] 4) aziridine carbaldehyde **6**,[11, 12] and 5) 1-amino-2-propanol. The ordering of steps a – e was not predetermined, although we had established the necessity of introducing the reactive azabicyclic system (bond d) as the penultimate step. The most relevant variable was the timing of the C7 – C8 dehydroamino acid olefination of aldehyde **6** (bond c) with respect to amide bond formations b and e. In other words, would the dehydroamino acid be introduced before or after elaboration of the amide/ester backbone?

[*] Prof. Dr. R. S. Coleman, Dr. J. Li, Dr. A. Navarro
Department of Chemistry
The Ohio State University
100 West 18th Avenue, Columbus, OH 43210-1185 (USA)
Fax: (+1) 614-292-4647
E-mail: coleman@chemistry.ohio-state.edu

[**] This work was supported by a grant from the National Cancer Institute (NIH CA-65875). A.N. was the recipient of a fellowship from the Spanish Ministerio de Educacion (EX0052672518). R.S.C. was an Alfred P. Sloan Foundation Research Fellow (1995 – 1998).

  1433-7851/01/4009-1736 $ 17.50+.50/0